A B



SLAC-PUB-6235
May 1993
(E)

# The NE11 Experiment at SLAC and the Neutron Form Factors*

L. M. Stuart,[2,4,a] A. Lung,[1,b] P. E. Bosted,[1] L. Andivahis,[1]
J. Alster,[12] R. G. Arnold,[1] C. C. Chang,[5] F. S. Dietrich,[4] W. R. Dodge,[7,c]
R. Gearhart,[10] J. Gomez,[3] K. A. Griffioen,[8] R. S. Hicks,[6] C. E. Hyde-Wright,[13]
C. Keppel,[1] S. E. Kuhn,[11,d] J. Lichtenstadt,[12] R. A. Miskimen,[6] G. A. Peterson,[6]
G. G. Petratos,[9,a] S. E. Rock,[1] S. H. Rokni,[6,a] W. K. Sakumoto,[9]
M. Spengos,[1] K. Swartz,[13] Z. Szalata,[1] L. H. Tao[1]

[1] *The American University, Washington D.C. 20016*
[2] *University of California, Davis, California 95616*
[3] *CEBAF, Newport News, Virginia 23606*
[4] *Lawrence Livermore National Laboratory, Livermore, California 94550*
[5] *University of Maryland, College Park, Maryland 20742*
[6] *University of Massachusetts, Amherst, Massachusetts 01003*
[7] *National Institute of Standards and Technology, Gaithersburg, Maryland 20899*
[8] *University of Pennsylvania, Philadelphia, Pennsylvania 19104*
[9] *University of Rochester, Rochester, New York 14627*
[10] *Stanford Linear Accelerator Center, Stanford, California 94309*
[11] *Stanford University, Stanford, California 94305*
[12] *University of Tel-Aviv, Ramat Aviv, Tel-Aviv 69978, Israel*
[13] *University of Washington, Seattle, Washington 98195*

*Presented at the 6th Workshop on Perspectives in Nuclear Physics at Intermediate Energies Trieste, Italy, May 3-7, 1993.*

* Work supported in part by National Science Foundation grants PHY–87–15050 (AU), PHY–89–18491 (Maryland), PHY–88–19259 (U Penn), and PHY–86–58127 (UW); by Department of Energy contracts DE–AC03–76SF00515 (SLAC), W–7405–ENG–48 (LLNL), DE–FG02–88ER40415 (U Mass), DE–AC02-ER13065 (UR) and DE–FG06–90ER40537 (UW) ; and by the US–Israel Binational Science Foundation. Present addresses: a) Stanford Linear Accelerator Center, Stanford, CA 94309 b) California Institute of Technology, Pasadena, CA 91125 c) George Washington University, Wash., D.C. 20052 d) Old Dominion University, Norfolk, VA 23529



## Abstract

Quasielastic $e$–$d$ cross sections have been measured over a large $\epsilon$ range for $Q^2$ = 1.75, 2.50, 3.25 and 4.00 (GeV/c)$^2$. Rosenbluth separations have been made on the cross sections to obtain $R_L$ and $R_T$ and the neutron form factors, $G_{En}$ and $G_{Mn}$, have been extracted via model dependent methods. The sensitivity of the form factor results to various model assumptions has been studied. The results for $G_{Mn}$ are consistent with form factor scaling, while $G_{En}$ is consistent with zero. Comparisons are made to several theoretical predictions.

## Introduction

The neutron electromagnetic form factors, $G_{En}$ and $G_{Mn}$, which reflect the charge and magnetization distributions within the neutron, are of fundamental importance for understanding nucleon structure, and are necessary for calculations of processes involving the electromagnetic interaction with complex nuclei. These quantities are functions of $Q^2$, the four-momentum transfer squared. SLAC experiment NE11 has measured these form factors out to a $Q^2$ of 4.0 (GeV/c)$^2$ with high precision, and the results have been recently published[1] This paper provides some additional details on the extraction of $G_{Mn}$ and $G_{En}$ from the NE11 measurements.

Several formalisms have been developed over the years which attempt to understand the nucleon form factors using basic physical principles. Vector Meson Dominance (VMD) models[2,3] are based on superpositions of photon couplings to various vector mesons. These models generally involve free parameters which are fit to form factor data at low $Q^2$, and are not expected to be valid at high $Q^2$. For asymptotically large $Q^2$, dimensional scaling methods[4] and perturbative Quantum Chromodynamics (pQCD)[5] predict form factor behavior at large $Q^2$, but they do not make absolute magnitude predictions. To describe the form factor behavior at intermediate values of $Q^2$, a hybrid model[6] by Gari and Krümpelmann (GK) uses VMD constraints at low $Q^2$ and pQCD constraints at high $Q^2$. Free parameters in the model are adjusted to fit existing form factor data. Other approaches include the use of QCD sum rules[7] to make absolute predictions, diquark models[8], and relativistic constituent quark models[9]

## Experiment

Previous measurements[10] of the elastic electron–neutron cross sections which depend on both $G_{En}$ and $G_{Mn}$ extend to $Q^2$ = 10 (GeV/c)$^2$, but separations of the

two form factors have only been made up to $Q^2 = 2.7$ (GeV/c)$^2$ with large errors.[11] These results are consistent with dipole scaling:

$$\frac{G_{Mn}(Q^2)}{\mu_n} = G_D(Q^2) = \frac{1}{(1 + Q^2/0.71)^2} \quad (1)$$

where $\mu_n = -1.913$ nm is the neutron anomalous magnetic moment. The present experiment, NE11, has made significant improvement to the experimental precision of the measured proton[12] and neutron[1] form factors as well as increasing the measured $Q^2$ range. The Nuclear Physics Injector at SLAC[13] provided beams with energies, $E$, ranging from 1.5 to 5.5 GeV and average currents from 0.5 to 10 $\mu$A. The beam angle and position were determined to within 0.05 mr and 1 mm, respectively using position sensitive resonant cavities and wire arrays. The total incident charge was measured by two independent toroidal charge monitors which agreed to within 0.2% and measured the absolute charge to 1%. The target consisted of a 15 cm long liquid deuterium cell which was 6.44 cm in diameter, with 0.1 mm thick aluminum walls and endcaps. A similar cell of liquid hydrogen was used to measure the $e$–$p$ cross sections for the proton form factor measurement, and a 1.8 mm thick aluminum target was used to measure endcap contributions. The liquid was circulated through the targets at 2 m/sec so that local density changes were negligible. The average density was determined from temperature-sensitive platinum resistors and vapor pressure bulbs with a run-to-run precision of 0.2% and an overall normalization of 0.9%.

Scattered electrons were measured simultaneously in two magnetic spectrometers. The SLAC 8 GeV/c spectrometer[14] detected electrons at central scattering angles, $\theta$, between 15° and 90°, and momentum between 0.5 and 7.5 GeV/c. The uncertainties in the 8 GeV spectrometer central momentum and angle were 0.05% and 0.005° respectively. The SLAC 1.6 GeV/c spectrometer[15] was upgraded for this experiment with two 10Q18 quadrupole magnets in order to increase its solid angle by nearly a factor of four. It was fixed at 90° which allowed for the use of tungsten slits to shield from the target endcaps. It measured cross sections with central momentum, $E'$, between 0.5 and 0.8 GeV/c. The uncertainty in the 1.6 GeV/c spectrometer angle was 0.05°. The optics of the 8 GeV/c spectrometer were better understood than those of the 1.6 GeV/c spectrometer due to a precision wire float calibration.[16] Therefore, the cross sections in the 1.6 GeV/c spectrometer were normalized to the 8 GeV/c data using a single normalization factor of 1.3% ± 1.0%.

Similar detector packages were used in each spectrometer to measure particle trajectories and to distinguish between electrons and background pions. The 8 GeV/c detectors consisted of a gas threshold Čerenkov counter filled with 0.6 atmospheres of nitrogen with an efficiency of 99.0%, ten planes of multi-wire proportional counters for particle tracking with a combined efficiency of 99.9%, and a lead glass shower counter array which had an efficiency of 99.4% and a resolution of $\pm 8\%/\sqrt{E'}$. The detector package also included two layers of scintillators for triggering purposes. The 1.6 GeV/c detectors consisted of a gas Čerenkov counter filled with $CO_2$ at atmosphere with an efficiency of 99.9%, twelve planes of drift chambers and four planes of scintillators for particle tracking with an efficiency of 99.0%, and a lead glass shower counter array with an efficiency of 98.2% and a resolution of $\pm 5\%/\sqrt{E'}$.



## Analysis

A Monte Carlo simulation of the spectrometer properties was used to generate the spectrometer acceptance as a function of relative momentum, $\delta$, relative horizontal scattering angle, $\Delta\theta$, and vertical scattering angle, $\phi$. The Monte Carlo was based on surveyed aperture information and on a TRANSPORT[17] model designed to agree with floating-wire[16] measurements of the optical coefficients. Two corrections to the acceptance function were also determined by the Monte Carlo. These corrections were for the momentum dependence of multiple scattering effects and for the change in effective target length when the spectrometer rotates about the pivot. The $\delta$-dependence of the acceptance function was checked by comparing deuterium inelastic cross sections measured at the same beam energy and scattering angle, but with the central spectrometer momenta differing by a few percent. Elastic $e$-$p$ cross sections were studied to verify that the acceptance function had no $\phi$-dependence and that the $\Delta\theta$ dependence did not differ from that expected from a global fit over a wide range of $\theta$. The Monte Carlo program for the 1.6 GeV/c spectrometer utilized a ray-trace model developed from fits to field gradient measurements in the quadrupoles and two and three-dimensional field calculations for the dipole which were checked against existing measurements. Acceptance checks similar to the ones described for the 8 GeV/c acceptance function were performed.

The measured counts were corrected for electronics and computer dead time and for the detector inefficiencies. Quasielastic $e$–$d$ spectra at each kinematic point were found as a function of $E'$ at fixed $\theta$ by dividing the corrected counts by the number of incident particles, the number of target particles per cm$^2$, and the acceptance function. The cross sections were also corrected for the small $\Delta\theta$ dependence of the cross section within the angular acceptance of the spectrometer using a model cross section. A correction of 0.85% was made to the cross sections due to hydrogen contamination in the deuterium target, and an average correction of 2% was made to the 8 GeV/c spectrometer cross sections for aluminum endcap contributions. Subtractions were also made for a background contamination of pions (typically 0.2%), and for electrons originating from pair-production in the target. The latter was measured in separate runs by reversing the polarity of the spectrometers, and was 3.5% in the worst case at $Q^2 = 4.0$ (GeV/c)$^2$ and $\theta = 90°$. Finally, radiative corrections were applied which were found using the peaking approximation formulas of Mo and Tsai[18,19]. The final radiative corrections were found using an iterative procedure where the input cross section model was adjusted after each iteration until convergence was obtained.

The measured $e$–$d$ cross sections per nucleon, $\sigma(E, E', \theta)$, were converted to reduced cross sections, defined as:

$$\sigma_R = \epsilon(1 + \tau')\frac{\sigma(E, E', \theta)}{\sigma_{Mott}} = R_T + \epsilon R_L \quad (2)$$

where $\sigma_{Mott} = \alpha^2 \cos^2(\theta/2)/4E^2 \sin^4(\theta/2)$, $\epsilon = [1 + 2(1 + \tau')\tan^2(\theta/2)]^{-1}$ is the longitudinal polarization of the virtual photon, with $\tau' = \nu^2/Q^2$, and $\nu = E - E'$.

Quasielastic spectra were measured over a large $\epsilon$ range (typically 0.2 to 0.9) for $Q^2$ = 1.75, 2.50, 3.25, and 4.00 (GeV/c)$^2$. There were four $\epsilon$ values for each of the two lowest $Q^2$ points, and three and two $\epsilon$ values for $Q^2$ = 3.25 and 4.00 (GeV/c)$^2$, respectively. The inelastic contribution at the quasielastic peak increased with $Q^2$ to a maximum of $\sim$ 15% at $Q^2$ = 4.00 (GeV/c)$^2$. Rosenbluth separations were done using linear fits to the reduced cross sections for each $W^2$ value at each $Q^2$. A normalized longitudinal response function, $R_L/G_D^2$, was obtained from the slope, and a transverse response function, $R_T/G_D^2$, from the intercept.

From this point on in the analysis, the neutron form factor extraction is model dependent. A comprehensive study has been made of this model dependence, and a summary is given here while further details are available.[20,21] Three different form factor extraction methods were implemented including two "area" methods. The first "area" method was a least-squares simultaneous fit to all the reduced cross section spectra at a given $Q^2$. The second was a similar fit applied separately to the extracted $R_L$ and $R_T$ spectra. A "peak" method of extraction was also done which only used data in the quasielastic peak region. This method is less sensitive to the modeling of the quasielastic peak shape, but the statistics are significantly reduced.

The shape of the quasielastic peak was modeled with a non-relativistic Plane Wave Impulse Approximation (PWIA) calculation[22] where the Paris,[23] Bonn,[24] and Reid soft-core[25] deuteron wave functions were all studied. In the PWIA, the quasielastic portion of $R_L$ is proportional to $(G_{Ep}^2 + G_{En}^2)$, and $R_T$ is proportional to $(G_{Mp}^2 + G_{Mn}^2)$. In addition to this nonrelativistic model, two sets of relativistic corrections were studied by Keister[26] and Gross.[27] The inelastic tail which extends under the quasielastic peak was modeled using a fit to the measured proton resonance region data which was convoluted with the deuteron wavefunction using a variety of Fermi-smearing models.[28,29] The smeared cross sections were fit to the deuterium data in the resonance region assuming two parameters: the ratio of neutron and proton cross sections, $\sigma_n/\sigma_p$, for resonance production, and for nonresonant background production. Several off-shell corrections which are applied to the input structure functions in the smearing models were also investigated.[30,31]

An effort was also made to estimate the effects due to meson-exchange currents (MEC). For the kinematic range of the NE11 data, no theoretical calculations were available for this effect. In lieu of these calculations, the MEC contribution was estimated using calculations made by Laget[32] for SLAC experiment NE4[33] at the largest $Q^2$ of 1.75 (GeV/c)$^2$. This $Q^2$ corresponds exactly to the lowest $Q^2$ NE11 point. The calculations included theoretical cross sections with and without contributions from MEC as well as final-state interactions (FSI), which were small compared to MEC. The difference in calculated reduced cross sections due to the MEC and FSI contributions was fit as a function of $W^2$ using a third degree polynomial fit. Results of this fit are shown in Figure 1. The cross sections were assumed to be purely transverse so that $R_L = 0.0$ and $\sigma_R = R_T^{MEC}$. The fit shown in Figure 1 was used for the shape of the (MEC + FSI) cross sections while the magnitude was a fit parameter.



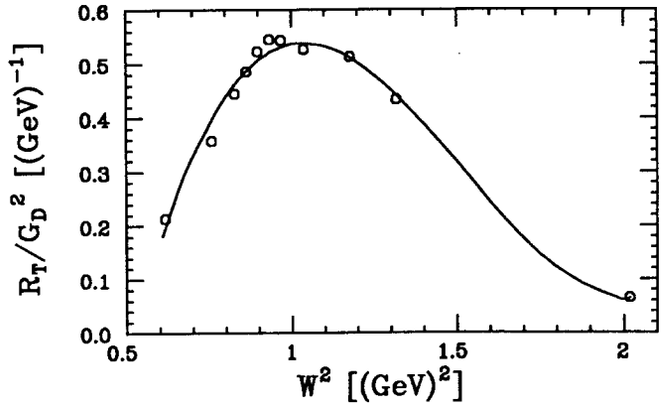


Figure 1. $R_T^{MEC}$ due to calculations by Laget[32] at $Q^2$ = 1.75 (GeV/c)$^2$. This contains both MEC and FSI contributions, but the FSI contributions are small. The curve is a fit to the calculations, and was used to describe the shape of the MEC and FSI contributions to the cross sections for the deuterium data fits.

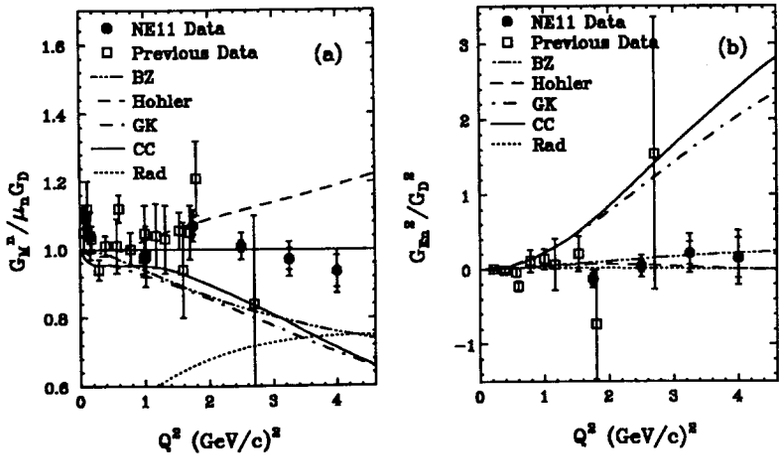


Figure 2. Results for a) $G_{Mn}/\mu_n G_D$ and b) $G_{En}^2/G_D^2$ versus $Q^2$ extracted using the "standard" model assumptions as described in text. The inner error bars are statistical, and the outer include systematic errors. Also shown are previous data and several theoretical curves: BZ[3], Hohler[2], GK[6], CC[9], and Rad[7].

## Results

All fits to the data yielded a measurement of the sum of the squares of the proton and neutron form factors. The neutron form factors were determined by subtracting the proton form factors measured in this experiment.[12] The results using "area" fit method 1, the Paris wave function, Keister relativistic corrections, the first smearing method as given by Sargsyan, Frankfurt and Strikman,[29] the off-shell correction given by Kusno and Moravczik,[31] and no MEC are shown in Figure 2. This choice of models will hereafter be referred to as "standard". In Figure 2 the inner error bars are statistical only, while the outer error bars include systematic errors. The point-to-point errors include the combined uncertainties in beam energy and scattering angle. The absolute systematic errors result from uncertainties in absolute values of the incident charge, radiative corrections, and solid angles of the spectrometers, as well as the absolute normalization of the proton form factors. Figures 2a and 2b show $G_{Mn}/\mu_n G_D$ and $G_{En}^2/G_D^2$ respectively, along with previous data and various theoretical predictions. The new data is in good agreement with previous data where there is overlap. None of the theoretical curves agree with the results for $G_{Mn}$, but dipole scaling is in agreement. The GK hybrid model (dash-dot) and the relativistic constituent quark model (CC, solid) both predict $F_{1n} = 0$, or $G_{En} = \tau G_{Mn}$ where $\tau = Q^2/4M^2$. This prediction is in very poor agreement with the new data for $G_{En}$. All of the remaining curves are in reasonable agreement with the $G_{En}$ data which is also consistent with zero for all the measurements. A careful study of the model dependence of the form factors indicates that most of the changes made to model variables produce negligible results. Table I summarizes the results of this study for $G_{Mn}$ variations from the "standard" model assumptions. In the approximate order of increasing influence we have deuteron wavefunctions, extraction fit methods, off-shell corrections, smearing methods, relativistic corrections and MEC effects. The first four of these are essentially negligible variations. The relativistic corrections of Gross[27] produce downward shifts of greater than one $\sigma$ for $G_{Mn}/\mu_n$, where $\sigma$ is the total error as shown in Figure 2. The MEC effects give large downward shifts on the order of two $\sigma$ for $G_{Mn}/\mu_n$. This indicates that further study on the MEC effect is warranted. A look again at Figure 2 shows that shifts this large will move the data points for $G_{Mn}$ down to agree with the theoretical curves BZ, CC, and GK. However, the simple method used here to estimate MEC effects could be giving anomalously large variations. Theoretical calculations for the kinematics of this experiment are needed to resolve this issue, and as of this date no such calculations are available. It should be noted, however, that adding the MEC effects improved the $\chi^2$ per degree of freedom for the fits to the data by roughly a factor of two and visibly filled in the "dip" region of the cross sections at the lowest $Q^2$. The "dip" region is located between the quasielastic peak and the $\Delta(1232)$ resonance peak. The model dependence for $G_{En}$ was essentially negligible within the experimental errors.



Table I. The quantity $(G_{Mn}(Q^2) - G_{Mn}^{Stan}(Q^2))/(\sigma(Q^2)\mu_n G_D)$ is shown here as a function of $Q^2$ and modeling variable. $G_{Mn}^{stan}(Q^2)$ are the results using the "standard" comparison model as described in the text and shown in Figure 2, $\sigma(Q^2)$ is the total error on $G_{Mn}(Q^2)$ and $Q^2$ is in $(\mathrm{GeV/c})^2$. The numbers indicate the maximum observed effect for each variable category

| | $Q^2$ 1.75 | $Q^2$ 2.50 | $Q^2$ 3.25 | $Q^2$ 4.00 |
|---|---|---|---|---|
| $D_2$ wave function | −0.17 | −0.15 | −0.04 | 0.09 |
| extraction method | −0.40 | −0.03 | 0.06 | 0.27 |
| off-shell corr. | −0.13 | −0.20 | −0.22 | −0.25 |
| smearing method | 0.13 | 0.25 | 0.37 | 0.47 |
| relativistic corr. | −0.66 | −1.10 | −1.24 | −0.95 |
| MEC effects | −1.98 | −1.63 | −2.45 | −2.91 |

## Conclusions

Quasielastic $e$–$d$ cross sections have been measured and Rosenbluth separations used to obtain $R_L$ and $R_T$, at $Q^2 = 1.75$, 2.50, 3.25 and 4.00 $(\mathrm{GeV/c})^2$. Using a PWIA model, values for $G_{En}$ and $G_{Mn}$ have been extracted which greatly increase the $Q^2$ range of previous data with significantly smaller error bars. Model studies indicate that there is some sensitivity to relativistic corrections and possibly a large sensitivity to MEC effects, but more work is needed for conclusive results. Assuming no MEC effects, the results for $G_{Mn}/\mu_n G_D$ are consistent with form factor scaling, and the results for $G_{En}^2/G_D^2$ are consistent with zero. None of the theoretical models agree well with both sets of form factor data. If the MEC effects are as big as these preliminary studies indicate then the results for $G_{Mn}/\mu_n G_D$ are significantly shifted down for all four data points, and the data agrees better with theoretical calculations. However, there is still no single model which adequately describes both the neutron and proton form factors. It is possible that use of the new data to adjust free parameters may improve agreement for many of the models.

## References

1. A. Lung *et al.*, Phys. Rev. Lett. **70**, 718 (1993).
2. G. Höhler *et al.*, Nucl. Phys. **B114**, 505 (1976). Fit 5.3.

3. S. Blatnik and N. Zovko, Acta. Phys. Austr. **30**, 62 (1974).
4. S. J. Brodsky and G. F. Farrar, Phys. Rev. D **11**, 1309 (1975).
5. G. P. Lepage and S. J. Brodsky, Phys. Rev. Lett. **43**, 545 (1979); **43**, 1625 (1979).
6. M. Gari and W. Krümpelmann, Z. Phys. **A322**, 689 (1985).
7. A. V. Radyushkin, Acta. Phys. Pol. **B15**, 403 (1984).
8. P. Kroll, M. Schürmann, and W. Schweiger, Z. Phys. **A338**, 339 (1991).
9. P. L. Chung and F. Coester, Phys. Rev. **D44**, 229 (1991). Model with $M_q = 0.24$.
10. S. Rock *et al.*, Phys. Rev. Lett. **49**, 1139 (1982).
11. W. Bartel *et al.*, Nucl. Phys. **B58**, 429 (1973).
12. P. E. Bosted *et al.*, Phys. Rev. Lett. **68**, 3841 (1992).
13. NPAS Users guide, SLAC Report No. 269, 1984 (unpublished).
14. P. N. Kirk *et al.*, Phys. Rev. D **8**, 63 (1973).
15. R. Anderson *et al.*, Nucl. Instr. Meth. **66**, 328 (1968).
16. L. Andivahis *et al.*, SLAC preprint SLAC–PUB–5753 (1992).
17. K. L. Brown, F. Rothacker, D. C. Carey, and Ch. Iselin, SLAC-Report- 91, Rev. 2 (1977).
18. L. W. Mo and Y. S. Tsai, Rev. Mod. Phys. **41**, 205 (1969).
19. Y. S. Tsai, SLAC-PUB-848 Rev. (1971), Rev. Mod. Phys. **46**, 815 (1974).
20. L. M. Stuart, Ph.D. Thesis, University of California, Davis (1992), UCRL-LR-110897.
21. A. Lung, Ph.D. Thesis, The American University (1992).
22. L. Durand III, Phys. Rev. **123**, 1393 (1961); I. J. McGee, Phys. Rev. **161**, 1640 (1967); **158**, 1500 (1967) as given by W. Bartel, *et al.*, Nucl. Phys. **B58**, 429 (1973).
23. M. Lacombe *et al.*, Phys. Lett. **101B**, 139 (1981).
24. R. Machleidt *et al.*, Phys. Rep. **149**, 1 (1987).
25. R. Reid, Ann. Phys. **50**, 411 (1968).
26. B. D. Keister, private communication. See also Phys. Rev. **C37**, 1765 (1988).
27. F. Gross and J. W. Van Orden, private communication. See also Phys. Rev. **C43**, 1022 (1991).
28. W. Atwood and G. West, Phys. Rev. D, **7**, 773 (1973).
29. M. M. Sargsyan, L. L. Frankfurt, and M. I. Strikman, Z. Phys. **A335**, 431 (1990).
30. A. Bodek, *et al.*, Phys. Rev. D, **20**, 1471 (1979).
31. D. Kusno and M. Moravczik, Phys. Rev. C, **27**, 2173 (1983).
32. J. M. Laget, Can. J. Phys. **62**,1046 (1984); J. M. Laget, Phys. Lett. B **199**, 493 (1987).
33. R. G. Arnold, *et al.*, Phys. Rev. Lett., **61**, 806 (1988).